01,05,07,15

# Peculiarities of resistivity and isothermal magnetization of manganese arsenide at high pressure

© T.R. Arslanov[1], L.N. Khanov[1], G.G. Ashurov[1], A.I. Ril[2]

[1] Amirkhanov Institute of Physics, Daghestan Federal Research Center, Russian Academy of Sciences, Makhachkala, Russia
[2] Kurnakov Institute of General and Inorganic Chemistry, Russian Academy of Sciences, Moscow, Russia

E-mail: arslanovt@gmail.com

*Received September 22, 2023*
*Revised November 29, 2023*
*Accepted November 30, 2023*

This paper presents an experimental study of the resistivity and isothermal magnetization of a bulk crystal MnAs under hydrostatic pressure that focuses on the development of its magnetic $P$-$T$ phase diagram. The pressure dependencies $\rho(P)$ and magnetization $M(P)$ reveal signatures for the new ferromagnetic MnAs phase at $P > 2.3$ GPa, different from the initial hexagonal one. The obtained results confirm the previous findings of neutron diffraction studies, suggesting the ferromagnetic MnAs phase with an orthorhombic structure above pressures of 2 GPa. It has been shown that at room temperature and high pressure ranges up to 8.5 GPa this phase remains stable.

**Keywords:** manganese arsenide, magnetization, magnetostriction, resistivity, high pressure.

DOI: 10.21883/0000000000

## 1. Introduction

Binary manganese pnictide compounds are formed due to stable chemical bond between subgroup 15 elements and transition group 7 element Mn. Since manganese has electronic configuration $4s^2 3d^5$, i. e. has five unpaired valence electrons on $d$ shell, then he resulting compounds exhibit magnetic properties after hybridization with three $p$ electrons of subgroup 15 elements (N, P, As, Sb, Bi). Among the known manganese pnictide compounds, manganese arsenide, MnAs, holds a special place due to its high potential in the energy-saving and environmentally-friendly cooling technology based on the magnetocaloric effect [1–5]. In addition, in recent decades, thin MnAs layers have been extensively used as element modules for spintronics devices owing to implementation of spin-polarized effects in MnAs/GaAs-based hybrid heterostructures [6,7].

Unique properties of MnAs mainly originate from the features of magnetic transformation of MnAs together with structural changes, and from rich magnetic phase diagram. Bulk MnAs in normal conditions has NiAs type hexagonal structure ($\alpha$-MnAs phase) which, with temperature rise, transforms into MnP type orthorhombic structure ($\beta$-MnAs phase) at the Curie temperature $T_C = 317$ K with a stepwise volume change of about $\sim 2\%$. This structural transition is followed by magnetic transformation from the ferromagnetic $\alpha$ phase into the paramagnetic $\beta$ phase with latent heat release and pronounced temperature hysteresis [8]. Orthorhombic distortion at $T_C$ approaches 1 and decreases gradually with further temperature rise resulting in the restoration of the hexagonal structure ($\gamma$-MnAs phase) at $T_t \sim 398$ K through the second-order phase transition.

Currently, the temperature-pressure phase diagram ($T$-$P$) of manganese arsenide is shown in [8] and [9]. The key findings of these papers suggest that the hexagonal ferromagnetic $\alpha$ phase becomes instable up to 4.6 kbar (1 kbar $\approx$ 0.1 GPa) and the orthorhombic $\beta$ phase prevails in a wide temperature range from 77 K to 500 K. Between pressures of 3 kbar and 4.6 kbar and at temperatures below 230 K, an orthorhombic structure with long-range antiferromagnetic order is formed and likely co-exists with the ferromagnetic order up to $\sim$ 50 K. At room temperature, the paramagnetic orthorhombic $\beta$ phase still prevails up to 20−25 kbar and may transform into the ferromagnetic state with pressure rise [10]. Thus, the literature data suggests that the magnetic phase $T$-$P$ diagram of MnAs was studied in a relatively small pressure range up to 3 GPa and, therefore, to define the boundaries of the orthorhombic ferromagnetic phase naturally necessitates an increase in the pressure range. Investigations of manganese arsenide properties in the higher pressure range become especially important in terms of recent detection of unusual superconductivity at $T_{SC} \approx 1$ K and $P \sim 8$ GPa in MnP [11,12].

Herein, we study the resistivity and isothermal magnetization of MnAs up to 8.5 GPa near room temperatures. The findings indicate that the ferromagnetic orthorhombic phase occurs at $P > 2.3$ GPa that remains stable up to maximum pressure used herein.

## 2. Samples and experimental procedure

Bulk polycrystalline MnAs samples were synthesized by the vacuum-ampoule from As and Mn taken at stoichiomet-

ric ratio [13]. The prepared samples were characterized by the powder X-ray diffraction using Bruker D8 Advance diffractometer ($\mathrm{Cu}\,K_\alpha$-radiation with $\lambda = 1.540\,\text{Å}$). Peaks corresponding to the hexagonal MnAs (space group $P63/mmc$) were identified on the diffraction profile. The following parameters of the MnAs lattice cell were defined: $a = 3.7063\,\text{Å}$ and $b = 5.7357\,\text{Å}$. Sample magnetization at atmospheric pressure was measured using SQUID magnetometer and detected a Curie temperature of $T_C = 317\,\text{K}$ in heating conditions, which is in agreement with the typical values of $T_C$ for MnAs. Thermal expansion was measured by the strain-gauge method [14] on $3 \times 3.5 \times 1.8\,\text{mm}^3$ samples.

Transport and magnetic properties at high pressure were measured using „Toroid-15“ high pressure unit within the hydrostatic compression up to 9 GPa [15]. Resistivity was measured using a standard four (contact) method on a sample wit typical dimensions $3 \times 1 \times 1\,\text{mm}^3$. Direct current flowing through the sample was 60 mA. Isothermal magnetization at high pressure was measured using he induction method. The measurement technique is described in detail the supplement to [16]. Methanol-ethanol mixture (4:1) was used as a pressure-transfer medium in a $\sim 80\,\text{mm}^3$ PTFE capsule. The pressure inside the capsule was controlled using a manganin sensor calibrated by reference phase transitions in Bi.

## 3. Findings and discussion

Properties of the prepared MnAs crystals at atmospheric pressure that mark a singularity at $T_C$ were examined using transport and thermophysical measurements. Figure 1 shows the resistivity-temperature dependence $\rho(T)$ of MnAs at $T = 190-350\,\text{K}$. Curves $\rho(T)$ measured in heating and cooling conditions at $T < 300\,\text{K}$ show that a metallic form of conductivity typical for MnAs prevails. At $T > 300\,\text{K}$, sharp resistivity changes in heating and cooling correspond to the phase transformations from $\alpha$-MnAs phase into $\beta$-MnAs phase and back. $T_C \approx 317\,\text{K}$ and $T_C \approx 308\,\text{K}$ or heating and cooling curves (defined as $d\rho/dT$), respectively, coincide with $T_C$ derived from the magnetization-temperature dependence of MnAs [16]. The temperature hysteresis with a width of $\Delta T \sim 9\,\text{K}$ between heating and cooling curves on $\rho(T)$ also implies the first-order magnetic transformation and is in good agreement with the findings of [17].

The hysteresis behavior of the MnAs resistivity at $T_C$ occurs on the thermal expansion-temperature dependence $\Delta l/l_0$ shown in Figure 2. The hysteresis region with applied 18 kOe magnetic field moves to the high temperature region with simultaneous decrease of $\Delta T$ (Detail in Figure 2) in accordance with the magnetic field effect on $T_C$ [18].

The view of the transverse magnetostriction - temperature dependence $\lambda_\perp$ measured in 18 kOe magnetic field as shown in Figure 3 suggests the prevailing magnetic bulk effect. Such behavior is associated with lambda magnetostriction anomaly at temperatures near $T_C$ in heating and

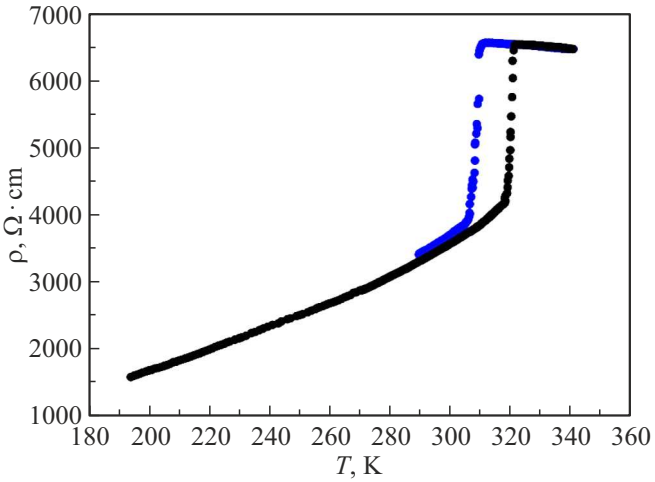


**Figure 1.** Dependence of MnAs resistivity on temperature in heating (black dots) and cooling (blue dots).

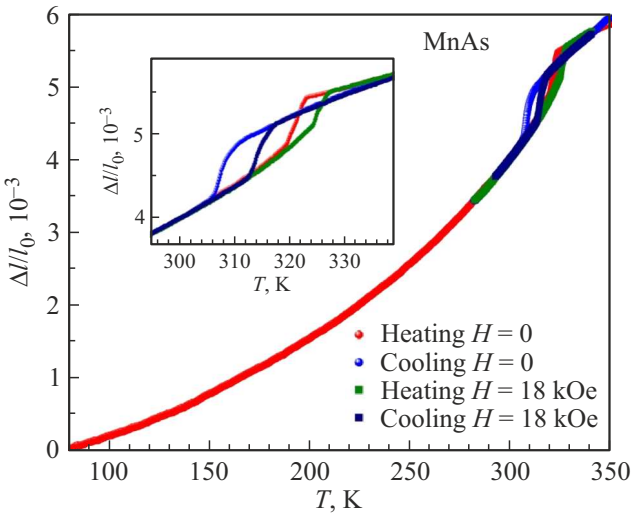


**Figure 2.** Thermal expansion-temperature dependence of MnAs measured in $H = 0$and and $H = 18\,\text{kOe}$ magnetic fields in heating and cooling. The Detail shows a scaled up hysteresis region $\Delta l/l_0$.

cooling. A minor difference between the minimum values $\lambda_\perp = -3.3 \cdot 10^{-5}$ and $\lambda_\perp = -3.97 \cdot 10^{-5}$ in heating and cooling may imply almost identical behavior of structural and magnetic variations in the $\alpha$-MnAs $\leftrightarrow$ $\beta$-MnAs transformation region.

It should be noted that the magnetic field effect on the $\alpha$-MnAs $\rightarrow$ $\beta$-MnAs transformation region results not only in the movement of $T_C$ towards the high temperature region, but also in the expected change of the phase transition order between the first and second order due to $\Delta T \rightarrow 0$ [18]. An opposite effect demonstrating that $T_C$ moves to the low temperature region is implemented under high pressure [19,20]. With an increase in pressure, the hexagonal structure of MnAs is destabilized at relatively low pressures with baric coefficients $-16.8\,\text{K/kbar}$ (heating) and $-25.1\,\text{K/kbar}$ (cooling) [20]. Following the magnetic $T$-$P$ phase diagram

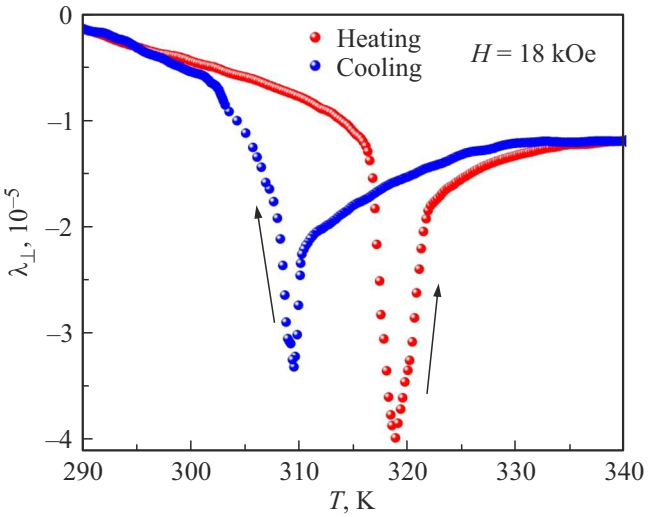


**Figure 3.** Dependence of MnAs magnetostriction on temperature in $H = 18$ kOe magnetic field in heating and cooling.

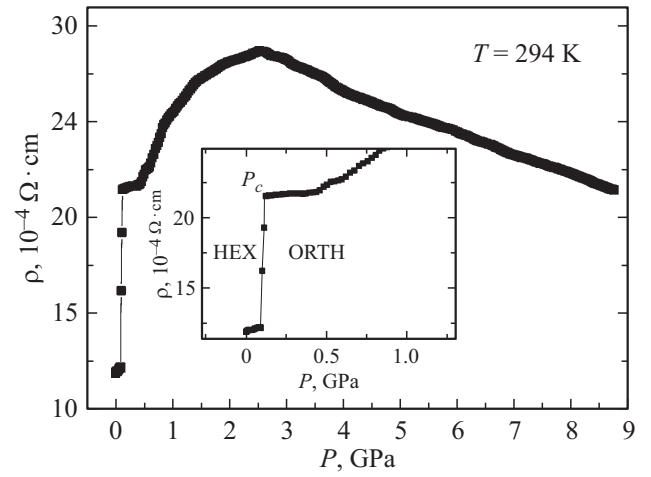


**Figure 4.** Dependence of the MnAs resistivity on pressure. The Detail shows the first phase transmission region in the low pressure range.

of MnAs [8], the orthorhombic ferromagnetic MnAs phase is emerging at $P > 8$ kbar and has a significant positive baric coefficient of $dT_C/dP$. According to these considerations, the new ferromagnetic MnAs phase boundary may cover the room temperature range when higher pressures are applied. Thus, direct measurements of pressure-sensitive parameters such as resistivity and magnetization may objectively imply that the orthorhombic ferromagnetic MnAs phase is observed in the room temperature region.

Figure 4 shows the resistivity-pressure dependence $\rho(P)$ measured at $T = 294$ K. The observed dramatic growth of $1\rho$ at $P \sim 0.12$ GPa suggests the phase transformation from the ferromagnetic hexagonal phase into the orthorhombic paramagnetic MnAs phase as shown in Detail in Figure 4. This transition is well reproducible and is in agreement with $\rho(P)$ measured in the pressure range up to 0.24 GPa in [9]. By increasing the pressure range up to 8.5 GPa, we recorded a qualitative variation of $\rho(P)$ behavior. The prevailing dome-shaped behavior with the peak at $P \approx 2.52$ GPa and then further monotonous decrease with an increase in pressure may indicate the occurrence of the second transformation from the paramagnetic orthorhombic state into ferromagnetic state of the same crystalline structure.

To verify the behavior of the observed transformations in MnAs, we have measured the isothermal magnetization as function of high pressure $M(P)$ shown in Figure 5. The observed singularities on $\rho(P)$ are clearly reflected in the behavior of $M(P)$ measured in similar temperature conditions ($T = 293$ K) with application of weak magnetic field 100 Oe. In particular, $M(P)$ demonstrates dramatic drop at $P \sim 0.12$ GPa indicating the pressure-induced transformation from $\alpha$-MnAs into $\beta$-MnAs phase. In the pressure region where the dome-shaped behavior of $\rho(P)$ prevails at $P \sim 2.3$ GPa, dramatic magnetization growth is observed and indicates the magnetic phase transition from the paramagnetic $\beta$-MnAs phase to the ferromagnetic $\beta$-MnAs phase. It is interesting that with further pressure growth, magnetization varies slightly suggesting that ferromagnetic ordering is stabilized in the orthorhombic phase up to 7 GPa. Thus, the measured dependence $M(P)$ confirms that the ferromagnetic $\beta$-MnAs state is being formed. In addition, as it follows from $\rho(P)$, this transformation is likely followed by the conductivity type variation from metallic to semiconductor type at $P > 2.52$ GPa. It should be noted that a decrease in $\rho$ with pressure growth is most common for the semiconductor conductivity type both for magnetic and nonmagnetic semiconductor compounds due to the decrease in the band gap width [21–25].

Based on these neutron investigations, it was shown in [26] that the ferromagnetic $\beta$-MnAs phase was really identified at 3.8 GPa and $T = 295$ K with magnetic moment $2.3\,\mu_B$ which is a little lower than $2.7\,\mu_B$ for the initial

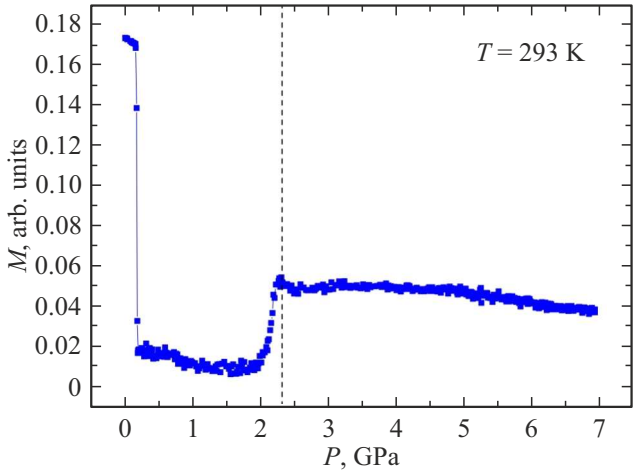


**Figure 5.** Dependence of the isothermal magnetization on pressure. The dashed line shows the start of the ferromagnetic $\beta$-MnAs phase.

ferromagnetic $\alpha$-MnAs phase. On the other hand, based on the expanded $T$-$P$ phase diagram of MnAs built from these magnetic measurements, the new ferromagnetic MnAs phase was reported to remain stable up to 3.2 GPa [10] and in accordance with the findings of [8] has a positive baric coefficient $dT_C/dP$. Our findings point out quite broad pressure range (up to 8.5 GPa), where high-pressure ferromagnetic $\beta$-MnAs phase may exist. It should be noted that to define the upper boundary of its phase region taking into account the positive coefficient $dT_C/dP$, isothermal measurements of the resistivity and magnetization shall be carried out at $T > 317$ K, i.e. above $T_C$. However, an increase in temperature conditions may create particular procedural difficulties associated with the properties variation of the pressure-transfer medium (methanol-ethanol mixture) resulting in violation of the pressure hydrostaticity condition. The use of other types of hydrostatic liquids, for example, glycerine-water mixture [27], may facilitate an increase in the measurement temperature range, but limits the pressure range up to 6 GPa. Therefore, to define the upper phase boundary of the ferromagnetic $\beta$-MnAs, apparently, it will be necessary to use alternative (quasi-hydrostatic) pressurization principles.

## 4. Conclusion

Experimental study of the resistivity and isothermal magnetization of MnAs was conducted at high pressures up to 8.5 GPa and room temperature. Based on the obtained data, magnetic and structural phase transformations induced by hydrostatic pressure have been identified. It is shown that, besides the well known transformation from $\alpha$-MnAs phase to $\beta$-MnAs phase at $P \sim 0.12$ GPa [9,10], the second orthorhombic ferromagnetic $\beta$-MnAs phase is formed at $P > 2.3$ GPa that have been previously observed in the neutron diffraction [26] and neutrol depolarization [28] experiments. In contrast to the initial metallic $\alpha$-MnAs phase, this phase has presumably a semiconductor type of conductivity. The new phase existence region extends to 8.5 GPa.

### Funding

This study was supported financially by the Russian Science Foundation (RSF) under project No. 23-22-00324.

### Conflict of interest

The authors declare that they have no conflict of interest.

## References

[1] H. Wada; Y. Tanabe. Appl. Phys. Lett. **79**, 3302 (2001).
[2] S. Gama, A.A. Coelho, A. de Campos, A. Magnus G. Carvalho, Flávio C.G. Gandra, P.J. von Ranke, N.A. de Oliveira. Phys. Rev. Lett. **93**, 237202 (2004).
[3] A. de Campos, D.L. Rocco, A.M.G. Carvalho, L. Caron, A.A. Coelho, S. Gama, L.M. da Silva, F.C.G. Gandra, A.O. dos Santos, L.P. Cardoso, P.J. von Ranke, N.A. de Oliveira. Nature Mater. **5**, 802 (2006).
[4] A.M. Aliev, L.N. Khanov, A.G. Gamzatov, A.B. Batdalov, D.R. Kurbanova, K.I. Yanushkevich, G.A. Govor. Appl. Phys. Lett. **118**, 072404 (2021).
[5] V.I. Mityuk, N.Yu. Pankratov, G.A. Govor, S.A. Nikitin, A.I. Smarzhevskaya. FTT **54**, *10*, 1865 (2012). (in Russian).
[6] P.N. Hai, S. Ohya, M. Tanaka, S.E. Barnes, S. Maekawa. Nature (London) **458**, 489 (2009).
[7] M. Tanaka. Semicond. Sci. Technol. **17**, 327 (2002).
[8] N. Menyuk, J.A. Kafalas, K. Dwight, J.B. Goodenough. Phys. Rev. **177**, 942 (1969).
[9] J.B. Goodenough, J.A. Kafalas. Phys. Rev. **157**, 389 (1967).
[10] I.F. Gribanov, E.A. Zavadsky, A.P. Scivachenko. FNT **5**, *10*, 1219 (1979). (in Russian).
[11] J.-G. Cheng, K. Matsubayashi, W. Wu, J.P. Sun, F.K. Lin, J.L. Luo, Y. Uwatoko. Phys. Rev. Lett. **114**, 117001 (2015).
[12] Y. Wang, Y. Feng, J.G. Cheng, W. Wu, J.L. Luo, T.F. Rosenbaum. Nature Commun **7**, 13037 (2016).
[13] S.F. Marenkin, A.V. Kochura, A.D. Izotov, M.G. Vasil'ev. Russ. J. Inorg. Chem. **63**, 1753 (2018).
[14] L.N. Khanov, A.M. Aliev, A.V. Mashirov. FTT **65**, *9*, 1560 (2023). (in Russian).
[15] L.G. Khvostantsev, V.N. Slesarev, V.V. Brazhkin. High Press. Res. **24**, 371 (2004).
[16] T.R. Arslanov, L.A. Saypulaeva, A.G. Alibekov, X.F. Zhao, A.I. Ril, S.F. Marenkin. Appl. Phys. Lett. **120**, 202406 (2022).
[17] A.T. Satya, E.P. Amaladass, A. Mani. Mater. Res. Express **5**, 046104 (2018).
[18] A.M.G. Carvalho, A.A. Coelho, S. Gama, F.C.G. Gandra, P.J. von Ranke, and N.A. de Oliveira. Eur. Phys. J. B **68**, 67 (2009).
[19] H. Wada, S. Matsuo, A. Mitsuda. Phys. Rev. B **79**, 092407 (2009).
[20] D.L. Rocco, A. de Campos, A.M.G. Carvalho, A.O. dos Santos, L.M. da Silva, S. Gama, M.S. da Luz, P. von Ranke, N.A. de Oliveira, A.A. Coelho, L.P. Cardoso, J.A. Souza. Phys. Rev. B **93**, 054431 (2016).
[21] F. Sun, N.N. Li, B.J. Chen, Y.T. Jia, L.J. Zhang, W.M. Li, G.Q. Zhao, L.Y. Xing, G. Fabbris, Y.G. Wang, Z. Deng, Y.J. Uemura, H.K. Mao, D. Haskel, W.G. Yang, C.Q. Jin. Phys. Rev. B **93**, 224403 (2016).
[22] K. Akiba, K. Kobayashi, T.C. Kobayashi, R. Koezuka, A. Miyake, J. Gouchi, Y. Uwatoko, M. Tokunaga. Phys. Rev. B **101**, 245111 (2020).
[23] A.G. Gamzatov, S.A. Gudin, T.R. Arslanov, M.N. Markelova, A.R. Kaul. Pisma v ZhETF **115**, *4*, 218 (2022). (in Russian).
[24] T.R. Arslanov, R.G. Dzhamamedov, V.S. Zakhvalinskii, A.V. Kochura, V.V. Rodionov, R. Ahuja. Appl. Phys. Lett. **115**, 252101 (2019).
[25] G. Zhang, B. Wu, J. Wang, H. Zhang, H. Liu, J. Zhang, C. Liu, G. Gu, L. Tian, Y. Ma, Ch. Gao. Sci Rep **7**, 2656 (2017).
[26] V.P. Glazkov, D.P. Kozlenko, K.M. Podurets, B.N. Savenko, V.A. Somenkov. Crystallography Rep. **48**, 54 (2003).
[27] V.A. Sidorov, O.B. Tsiok. Fizika i tekhnika vysokikh davleniy, **1**, *3*, 74 (1991). (in Russian).
[28] K.M. Podurets, S.A. Klimko, V.V. Runov, V.A. Somenkov, V.P. Glazkov. Physica B **297**, 258 (2001)

*Translated by E.Ilinskaya*